ECA 2021

sciforum

Conference Proceedings Paper

An Insight Into the Potentiation Effect of Potassium Iodide on aPDT Efficacy†

Cátia Vieira[1], Ana T. P. C. Gomes[1]*, Mariana Q. Mesquita[2], Nuno M. M. Moura[2], M. Graça P. M. S. Neves[2], M. Amparo F. Faustino[2]* and Adelaide Almeida[1]*

[1] Department of Biology and CESAM, University of Aveiro, Aveiro, Portugal;
[2] Department of Chemistry and LAQV-REQUIMTE, University of Aveiro, Aveiro, Portugal;
gtino@ua.pt; Adelaide Almeida, email: aalmeida@ua.pt.
† Presented at the 1st International Electronic Conference on Antibiotics—The Equal Power of Antibiotics and Antimicrobial Resistance, 8–17 May 2021; Available online: https://eca2021.sciforum.ne

Abstract: Antimicrobial photodynamic therapy (aPDT) is an effective approach against multidrug-resistant strains. The addition of potassium iodide (KI), a non-toxic salt, is recognized to increase the aPDT efficiency of some photosensitizers (PSs) on a broad-spectrum of microorganisms. To gain a more comprehensive knowledge about the PS and KI combined effect, in this work we assessed the effect of KI in the presence of a broad range of porphyrinic and non-porphyrinic PSs against a bioluminescent *Escherichia coli* strain used as a bacterial model. The results indicate that KI can potentiate the aPDT mediated by some cationic PSs, allowing a drastic reduction of the aPDT treatment time and PS concentration. However, the efficacy of some porphyrinic and non-porphyrinic PSs was not improved. This study highlights that the PSs capable of decomposing the peroxyiodide into iodine, are the most promising ones to be used in combination with KI. Although this study confirms that $^1O_2$ generation is an important factor for the success of aPDT potentiation by KI, the PS structure, aggregation behavior and cell membrane affinity are also important features to consider.

Keywords: antimicrobial photodynamic therapy; porphyrins; phenothiazines; potassium iodide; bioluminescent *E. coli*

1. Introduction

Antibiotics are commonly prescribed drugs in both human medicine and farm animals, resulting in the selection of multiple drugs resistant (MDR) bacteria [1]. Infections with resistant bacteria are difficult to treat, causing severe illness and requiring alternative and efficient approaches for their control [2].

Antimicrobial photodynamic therapy (aPDT) is a promising alternative to the conventional treatments [3] that involves the use of a photosensitizer (PS) which in the presence of visible light and dioxygen produces reactive oxygen species (ROS), such as singlet oxygen ($^1O_2$). These ROS are responsible for the oxidation of several cellular components conducting to the microbial inactivation [4].

Recently, some studies have demonstrated that the addition of potassium iodide (KI), a non-toxic salt, can enhance the aPDT efficiency on a broad-spectrum of microorganisms [5-12]. The combination of this salt with some PSs improves the microbial inactivation rates, when compared to the PSs alone. The mechanism of action involved in this enhanced killing effect is caused by parallel reactions initiated by the reaction of $^1O_2$ with KI, to produce peroxyiodide. In turn, peroxyiodide may suffer further decomposition by two different pathways: formation of free iodine (I_2/I_3^-) and hydrogen peroxide (H_2O_2); or through a homolytic cleavage process in which reactive iodine radicals ($I_2^{\cdot-}$) are produced [5-12].

Considering that most of the studies reported in the literature refer a positive aPDT potentiation by KI, we decided to gain a more comprehensive knowledge about this type of effect by evaluating the photodynamic action of a broad range of cationic porphyrinic and non-porphyrinic dyes as PSs towards a bioluminescent *E. coli* strain in the presence of KI [13]. The structures of the selected PSs are summarized in **Figure 1** and comprise: (i) the five structurally related cationic *meso*-tetraarylporphyrins: **Mono-Py(+)-Me**, **Di-Py(+)-Me** ***opp*** and **Di-Py(+)-Me** ***adj***, **Tri-Py(+)-Me** and **Tetra-Py(+)-Me** [14]; a formulation (**Form**) based on the mixture of the previous 5 porphyrins [15]; and the neutral porphyrin *meso*-tetra(4-pyridyl)porphyrin (**Tetra-Py**) [14] (ii) the three β-substituted porphyrin derivatives **β-ImiPhTPP**, **β-ImiPyTPP**, and **β-BrImiPyTPP** bearing positively charged imidazole units [16]; and (iii) the non-porphyrinic dyes – methylene blue (**MB**), Rose Bengal (**RB**),Toluidine Blue O (**TBO**), crystal violet (**CV**) and malachite green (**MG**). The selection of these three PS series was based on their different photoinactivation profiles towards *E. coli* and their mechanisms of action (Mechanism of Type I or II).

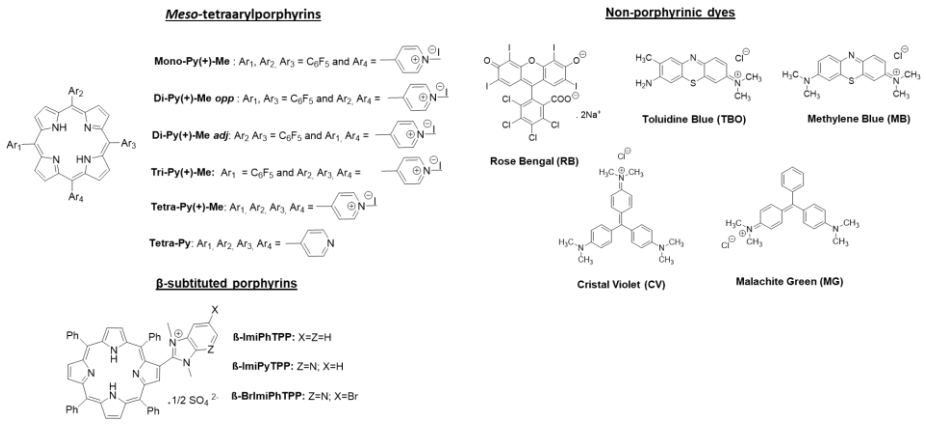

Figure 1. Structures and acronyms/abbreviations of the PSs used in this study.

2. Materials and Methods

2.1. Stock Solutions of Photosentitizers and bacterial strain:

The *meso*-tetraarylporphyrins [**Mono-Py(+)-Me**, **Di-Py(+)-Me** ***opp***, **Di-Py(+)-Me** ***adj***, **Tri-Py(+)-Me** and **Tetra-Py(+)-Me**], the porphyrinic formulation of the previous 5 non-separated porphyrins (**Form**), the neutral **Tetra-Py** and the β-substituted porphyrins **β-ImiPhTPP**, **β-ImiPyTPP**, and **β-BrImiPyTPP** were prepared accordingly with the literature [14-16]. **CV** was purchased from Merck, **RB** from Fluka AG, **MG** from Riedel-de-HaënTM, **MB** and **TBO** from Acros Organics. Stock solutions of each porphyrin and non-porphyrin dyes were prepared at 500 μM in dimethyl sulfoxide (DMSO) and in the phosphate buffer solution (PBS), respectively.

2.2. Antimicrobial Photodynamic Therapy (aPDT) Procedure:

The genetically transformed bioluminescent *E. coli* Top10 [17] was kept on Tryptic Soy Agar (TSA, Merck) at 4 °C. Before each assay, a fresh culture was obtained by subculturing in Trypic Soy Both (TSB, Merck), followed by overnight incubation at 25 °C under stirring, till stationary growth phase was achieved.

Bacterial suspensions of *E. coli* were tenfold diluted in PBS and equally distributed in 50 mL beakers. The assays were carried out by exposing the bacterial suspension to each PS (5.0 μM), either alone or combined with KI at 100 and 50 mM, and also at 25 mM for the **RB**, **CV**, **MG**. Light and dark controls were also carried out simultaneously with the aPDT procedure: the light controls comprised a bacterial suspension (LC-Bacteria) and a bacterial suspension with KI, at 100 mM (LC-KI), both exposed to light; and the dark control (DC) comprised a bacterial suspension incubated with the PSs and KI, at 100 mM, protected from light. The samples were incubated in the dark for 15 min to promote the PS binding to *E. coli* cells, and then were exposed to artificial white light (PAR radiation,

13 fluorescent lamps OSRAM 21 of 18 W each), at 25 W.m^{-2}, under stirring. Finally, aliquots of samples and controls were collected at different times of light exposure and the bioluminescence signal was measured in the luminometer. The assays were finished whenever the detection limit of the luminometer was achieved (*c.a* 2.3 log). Data were graphed from at least three independent experiments with two replicates of each condition.

2.3. Detection of Iodine Formation:

In a 96 wells microplate, solutions of each PS, at 5.0 μM, either alone or combined with KI, at 100 mM, were irradiated with white light at an irradiance of 25 W.m^{-2}. The generation of iodine was monitored by reading the absorbance at 340 nm during 120 min of irradiation.

3. Results and Discussion

Considering that two different pathways can be responsible for the extra bacterial killing when KI is combined with several PSs, it was assumed, as proposed in previous aPDT studies, that some information can be taken by the profile of inactivation [5-12]. If the inactivation curve shows a sharp decrease, free iodine (I_2/I_3^-) is the main killing species. Instead, if there is a gradual increase in killing, then there is a contribution from short-lived reactive iodine species. Bearing this in mind, we tried to explain the results obtained accordingly to the inactivation profile of *E. coli* observed for each combination of KI and PS, as summarized in **Table 1.** These results allowed us to classify the studied PSs in the following groups: (a) PSs in which their efficiency was potentiated by KI, being observed a gradual decrease in the *E. coli* survival profile [**Mono-Py(+)-Me**, **β-ImiPhTPP**, **β-ImiPyTPP**, and **β-BrImiPyTPP**]; (b) PSs in which their efficiency was potentiated by KI, being observed an abrupt decrease in the *E. coli* inactivation profile [**Tri-Py(+)-Me**, **Tetra-Py(+)-Me**, **Form**, **RB**, and **MB**]; and (c) PSs in which their efficiency was not potentiated by the addition of KI [**Di-Py(+)-Me *opp***, **Di-Py(+)-Me *adj***, **Tetra-Py**, **TBO**, **CV**, and **MG**].

Table 1. Results obtained in the photoinactivation of bioluminescent *E. coli* using combinations of tested PSs and KI. The results are organized accordingly to killing profile caused by KI.

	PS	Does KI potentiate aPDT?	Does KI causes a sharp decrease in the *E. coli* survival?
(a)	**Mono-Py(+)-Me**	√	X
	***β*-ImiPhTPP**	√	X
	***β*-ImiPyTPP**	√	X
	***β*-BrImiPhTPP**	√	X
(b)	**Tri-Py(+)-Me**	√	√
	Tetra-Py(+)-Me	√	√
	FORM	√	√
	MB	√	√
	RB	√	√
(c)	**Di-Py(+)-Me *opp***	X	N/A
	Di-Py(+)-Me *adj*	X	N/A
	TBO	X	N/A
	CV	X	N/A
	MG	X	N/A

1. √, yes ; X, no ; N/A, Not Applicable;
2. ***(a)*** PSs efficiency was potentiated by KI, with a gradual decrease in the *E. coli* survival profile; ***(b)*** PSs efficiency was potentiated by KI, with an abrupt decrease in the *E. coli* survival profile; ***(c)*** PSs efficiency was not potentiated by KI.

As demonstrated in **Figure 2**, we assume that the mechanism of action resultant of the combination of KI with the PSs **Mono-Py(+)-Me** (**Figure 2a**), **β-ImiPhTPP**, **β-ImiPyTPP**, and **β-BrImiPyTPP** (results demonstrated by Vieira *et al.* [13]), is probably associated to the formation of

iodine radicals ($I_2^{\bullet-}$) that, due to their short diffusion distance, cause a gradual decrease in the photoinactivation profile of *E.coli*. In the case of **Tetra-Py(+)-Me** (**Figure 2 b**), and of **Tri-Py(+)-Me**, **Form**, **MB** and **RB** (summarized in the study of Vieira *et al.* [13]), the preferential decomposition of the peroxyiodide leads to the formation of free iodine (I_2/I_3^-), which contributes significantly for the abrupt increase observed in the photoinactivation profile of the *E. coli* (**Figure 2 b**). This fact was confirmed by the formation of iodine (I_2/I_3^-), which was detectable by spectroscopy. In fact, as demonstrated in **Figure 3**, the PSs that cause a sharp decrease in the *E. coli* survival rate profile revealed higher ability to produce I_2 (**Figure 3 a**). On the other hand, the belatedly detection of I_2 was observed for PSs that cause a gradual decrease in the *E. coli* survival rate profile (**Figure 3 b**).

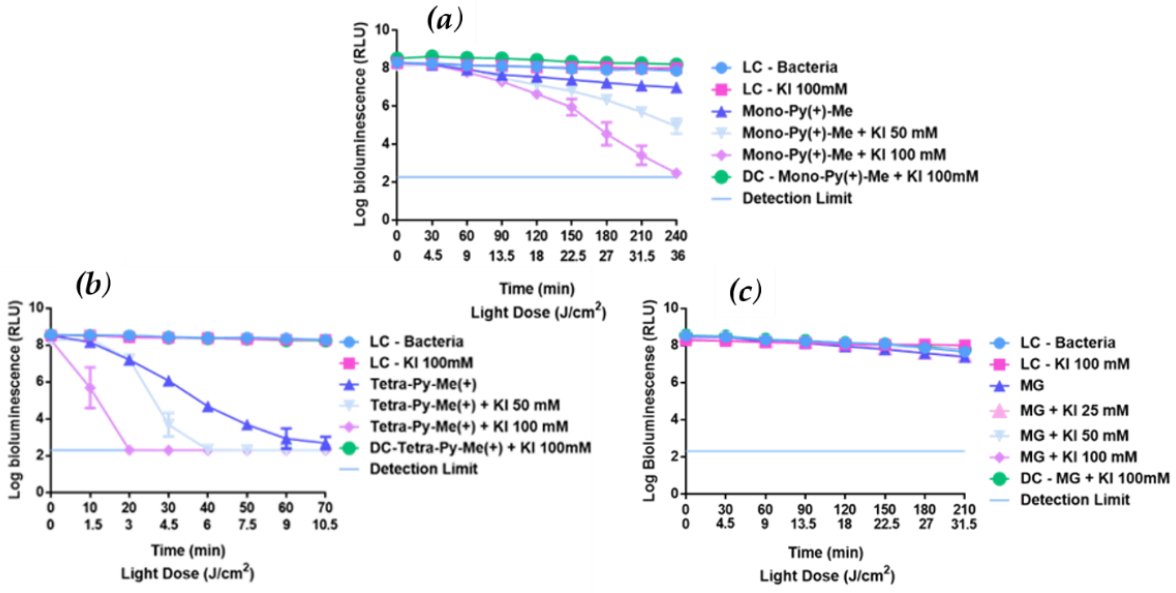

Figure 2. Differential survival profile of *E. coli* during aPDT assays in the presence of **Mono-Py(+)-Me** (a), **Tetra-Py(+)-Me** (b) and **MG** (c), at 5.0 μM, alone or combined with KI.

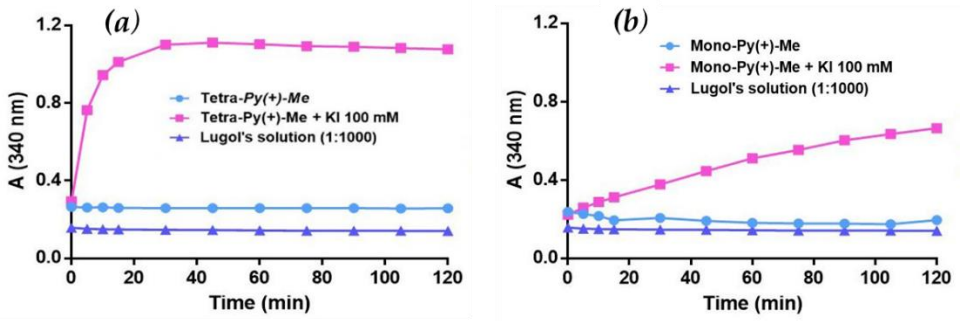

Figure 3. Monitoring of the formation of iodine, at 340 nm, after different irradiation periods in the presence of **Tetra-Py(+)-Me** (a) and **Mono-Py(+)-Me** (b), at 5.0 μM, and combinations of each PS, at 5.0 μM, and KI, at 100 mM.

In regard to PSs **Di-Py(+)-Me *opp***, **Di-Py(+)-Me *adj***, **Tetra-Py**, **TBO**, **CV** (results demonstrated in Vieira *et al.*, 2018 [13]) and **MG** (**Figure 2 c**) in which the efficiency was not potentiated by KI, or was even reduced, other factors that may contribute to this behavior should be considered. As demonstrated by Vieira *et al.* [13], the different behavior observed with the dicationic PSs **Di-Py(+)-Me *opp*** (the efficacy was lost in the presence of KI) and **Di-Py(+)-Me *adj*** (no potentiation with KI), is probably related with their different charge distribution across the molecule, since both isomers have similar high capability to generate $^1O_2$. Although both compounds are able to promote the formation of iodine radical species ($I_2^{\bullet-}$), in the case of **Di-Py(+)-Me *opp*,** these radicals, with a short diffusion distance, probably were not generated close enough to the target cells and the depletion of $^1O_2$ by the previous reaction was responsible by losing its former efficacy. On the other hand, for **Di-**

Py(+)-Me *adj*, the formation of toxic radicals in close proximity to the target cells can justify the maintenance of its efficacy. In the case of the neutral porphyrin, the results summarized in the study of Vieira *et al.* 2018 [13] revealed that **Tetra-Py** was inefficient to photoinactivate *E. coli*, even with KI, which can be explained by its tendency to aggregate in aqueous media, making it difficult to act as a PS. Regarding the non-porphyrin dyes, **CV** is known to produce a low yield of $^1O_2$, acting mainly through an electron-transfer mechanism (Type I) of aPDT. In contrast, **MG** do not produce $^1O_2$, acting only by the Type I mechanism. The results exhibited in the work carried out by Vieira *et al.* [13] clearly indicate their low efficiency in the photoinactivation of *E. coli*, either when acting alone or combined with KI, thus proving the importance of $^1O_2$ generation in the potentiation of aPDT processes mediated by KI. On the other hand, **TBO** acts mainly by Type II mechanism of aPDT and has a high capability of generating $^1O_2$. As demonstrated by Vieira *et al.* [13], when TBO acts alone, it is able to efficiently inactivate the bacteria. Nonetheless, its combination with KI does not potentiate its photodynamic activity towards *E coli* [13]. The improvement of the photodynamic action of **TBO** by KI was previously reported, but only when using concentrations 20 times higher than the one we tested (100 μM *versus* 5.0 μM) [18]. The different experimental conditions can then justify the differences observed in these two studies.

4. Conclusions

It is undeniable that the ability of KI to potentiate the aPDT process mediated by some cationic PSs, allows a drastic reduction of the aPDT treatment time, as well as the reduction of the PS concentration. However, this potentiation is limited to some PSs, and the addition of KI, may even impair some PSs. This work helped to elucidate that, among the studied compounds, the PSs capable of decomposing the peroxyiodide into iodine, are the promising ones in terms of complementing their efficacy with the action of iodine. Although these studies confirm that the generation of $^1O_2$ is an important factor in this process, the PS structure, its aggregation behavior and affinity for the cell membrane are also important features to consider.

Acknowledgments: Thanks are due to the University of Aveiro and FCT/MCTES for the financial support to CESAM (UIDP/50017/2020+UIDB/50017/2020) and LAQV-REQUIMTE (UIDB/50006/2020), to the FCT project PREVINE (FCT-PTDC/ASPPES/29576/2017), through national funds and when applicable co-financed by the FEDER, within the PT2020 Partnership Agreement and "Compete" 2020. Thanks are also due to the Portuguese NMR and Mass Networks. M.M. and C.V. thanks FCT for their doctoral grant (SFRH/BD/112517/2015) and (SFRH/PD/150358/2019), respectively, and N.M. thanks for his post-doctoral grant (SFRH/BPD/84216/2012).

Conflicts of Interest: The authors declare no conflict of interest.

References

3.

4. 1 - O'Neill, J. Tackling drug-resistant infections globally: final report and recommendations, in *The Review on Antimicrobial Resistance*, ed. A. Ro; HM Government and the Wellcome Trust: London, England, **2016**, *84*.
5. 2 - Wang, R.; Dorp, L.V.; Shaw, L.P.; Bradley, P.; Wang, Q.; Wang, X.; et al. The global distribution and spread of the mobilized colistin resistance gene Mcr-1. *Nat. Commun*. **2018**, *9*, 1–9. doi: 10.1038/s41467-018-03205-z.
6. 3 - Dai, T.; Huang, Y.Y.; Hamblin, M.R. Photodynamic therapy for localized infections – state of the art. *NIH Public Access*. **2010**, *6*, 170–188. doi: 10.1016/j.pdpdt.2009.10.008.
7. 4 - Jori, G.; Camerin, M.; Soncin, M.; Guidolin, L.; Coppellotti, O. Antimicrobial photodynamic therapy: basic principles, in *Photodynamic Inactivation of Microbial Pathogens?: Medical and Environmental Applications*, eds M. R. Hamblin and G. Jori (London: Royal Society of Chemistry), **2011**, 1–18. doi: 10.1039/9781849733083-0000.

8. 5 – Huang, L.; Szewczyk, G.; Sarna, T.; Hamblin, M.R. Potassium iodide potentiates broad-spectrum antimicrobial photodynamic inactivation using photofrin. *ACS Infect. Dis.* **2017**, *3*, 320–328. doi: 10.1021/acsinfecdis.7b00004
9. 6 – Huang, L.; El-Hussein, A.; Xuan, W.; Hamblin, M.R. Potentiation by potassium iodide reveals that the anionic porphyrin TPPS4 is a surprisingly effective photosensitizer for antimicrobial photodynamic inactivation. *J. Photochem. Photobiol. B Biol*. **2018**, *178*, 277–286. doi: 10.1016/j.jphotobiol.2017.10.036
10. 7 – Huang, Y.Y.; Wintner, A.; Seed, P. C.; Brauns, T.; Gelfand, J. A.; Hamblin, M.R. Antimicrobial photodynamic therapy mediated by methylene blue and potassium iodide to treat urinary tract infection in a female rat model. *Sci. Rep.* **2018**, *8*, 7257. doi: 10.1038/s41598-018-25365-0
11. 8 – Reynoso, E.; Quiroga, E; Agazzi, M.L.; Ballatore, M.B.; Bertolotti, S.G.; Durantini, E.N. Photodynamic inactivation of microorganisms sensitized by cationic BODIPY derivatives potentiated by potassium iodide. *Photochem. Photobiol. Sci.* **2017**, *16*, 1524–1536. doi: 10.1039/c7pp00204a
12. 9 – Wen, X.; Zhang, X.; Szewczyk, G.; El-Hussein, A.; Huang, Y.Y.; Sarna, T.; et al. Potassium iodide potentiates antimicrobial photodynamic inactivation mediated by rose bengal in in vitro and in vivo studies. *Antimicrob. Agents Chemother.* **2017**, *61*, e00467-17. doi: 10.1128/AAC.00467-17
13. 10 - Gsponer, N.S.; Agazzi, M.L.; Spesia, M.B.; Durantini, E.N. Approaches to unravel pathways of reactive oxygen species in the photoinactivation of bacteria induced by a dicationic fulleropyrrolidinium derivative. *Methods*. **2016**, *109*, 167–174. doi: 10.1016/j.ymeth.2016.05.019
14. 11 - Hamblin, M.R. Potentiation of antimicrobial photodynamic inactivation by inorganic salts. Expert Rev. *Anti Infect. Ther*. **2017**, *15*, 1059–1069. doi: 10.1080/14787210.2017.1397512.
15. 12 - Kashef, N.; Huang, Y.Y.; Hamblin, M.R. Advances in antimicrobial photodynamic inactivation at the nanoscale. *Nanophotonics*. **2017**, *6*, 853–879. doi:10.1515/nanoph-2016-0189
16. 13 - Vieira, C; Gomes, A.T.P.C; Mesquit, M.Q., Moura, N.M.M.; Neves, M.G.P.M.S.; Faustino, M.A.F; Almeida, A. An Insight Into the Potentiation Effect of Potassium Iodide on aPDT Efficacy. *Front. Microbiol*. **2018**, *9*, 2665. doi: 10.3389/fmicb.2018.02665
17. 14 – Simões, C.; Gomes, M.C.; Neves, M.G.P.M.S.; Cunha, A.; Tomé, J.P.C.; Tomé, A.C.; et al. Photodynamic inactivation of *Escherichia coli* with cationic meso-tetraarylporphyrins - the charge number and charge distribution effects. *Catal. Today*. **2016**, *266*, 197–204. doi: 10.1016/j.cattod.2015.07.031
18. 15 – Marciel, L.; Rosalina, F.; Ana, M.; Mariana, M.; Neves, M.G.P.M.S.; Adelaide, A. An efficient formulation based on cationic porphyrins to photoinactivate Staphylococcus aureus and *Escherichia coli*. *Future Med. Chem*. **2018**, *10*, 1821–1833. doi: 10.4155/fmc-2018-0010
19. 16 – Moura, N.M.M.; Esteves, M.; Vieira, C.; Rocha, G.M.S.R.O.; Faustino, M.A.F.; Almeida, A.; et al. Novel b-functionalized mono-charged porphyrinic derivatives: synthesis and photoinactivation of *Escherichia coli*. *Dyes Pigments*. **2019**, *160*, 361–371. doi: 10.1021/acs.chemrev.6b00427
20. 17 - Alves, E.; Carvalho, C.M.B.; Tomé, J.P.C.; Faustino, M.A.F.; Neves, M.G.P.M.S.; Tomé, A. C.; et al. Photodynamic inactivation of recombinant bioluminescent *Escherichia coli* by cationic porphyrins under artificial and solar irradiation. *J. Ind. Microbiol. Biotechnol*. **2008**. *35*, 1447–1454. doi: 10.1007/s10295-008-0446-2
21. 18 - Ghaffari, S.; Sarp, A.S.K.; Lange, D.; Gülsoy, M. Potassium iodide potentiated photodynamic inactivation of enterococcus faecalis using toluidine blue: comparative analysis and post-treatment biofilm formation study. *Photodiagnosis Photodyn. Ther.* **2018**, *24*, 245–49. doi: 10.1016/j.pdpdt.2018.09019
22.